



## Generated heat by different targets irradiated by 660 MeV protons

J Svoboda<sup>a,b,\*</sup>, J Adam<sup>a,b</sup>, S Foral<sup>b</sup>, S A Gustov<sup>a</sup>, K Katovsky<sup>b</sup>, J Khushvaktov<sup>a,e</sup>,  
D Kral<sup>b</sup>, A A Solnyshkin<sup>a</sup>, P Tichy<sup>a,c,d</sup>, S I Tyutyunnikov<sup>a</sup> & M Zeman<sup>a,b</sup>

<sup>a</sup>Joint Institute for Nuclear Research, Joliot-Curie 6, Dubna 141 980, Russia

<sup>b</sup>Faculty of Electrical Engineering and Communication, Brno University of Technology,  
Technicka 3058/10, Brno, 61600, Czech Republic

<sup>c</sup>Faculty of Nuclear Sciences and Physical Engineering, Czech Technical University in Prague,  
Brehova 7, 11519 Prague, Czech Republic

<sup>d</sup>Nuclear Physics Institute of the ASCR PRI, Hlavni 130, Rez near Prague 25068, Czech Republic

<sup>e</sup>Institute of Nuclear Physics ASRU, Ulugbek, Tashkent 100214, Uzbekistan

Received 17 February 2020

Calorimetric experiments have been performed to analyze different thick targets of <sup>nat</sup>U, C, Pb material, irradiated by 660 MeV protons at the Phasotron accelerator facility, Joint Institute for Nuclear Research (JINR) in Dubna, Russia. The method of online temperature measurement has been compared with MCNPX 2.7.0 simulation and selected with Ansys Transient Thermal Simulation to compare measured temperature with the simulated one. Thermocouples type T and E have been used as a temperature probe. Many different positions have been measured for each target. Temperature results are following very well the processes inside of the cylinders. Changes of heat deposition caused by drops of the proton beam intensity are displayed very well as a jagged line shown in almost every chart. Accurate temperature changing measurement is a very modest variation of how to observe inner macroscopic behavior online.

**Keywords:** ADS, MCNPX, ANSYS, Temperature measurement, Heat deposition, Thick target, Proton irradiation

### 1 Introduction

This paper is aimed to study the heat generation distribution of different targets from natural uranium, lead, and carbon material. Natural uranium experiments are discussed more detailly due to the long previous gamma spectroscopic research by our group dealing with ADS research. The motivation for this research is to continue with previous research performed at the end of the '90s and beginning of millennia in JINR by Batin, Tumendelger, Krivopustov, Voronkov, *et al.*, respectively<sup>1-4</sup>. These experimental researches were mostly implemented in the Synchrophasotron irradiation facility at JINR or either in U-70 accelerator facility at Institute for High Energy Physics, Protvino. For the last five years, our ADS group has met with the opportunity to implement experimental research at the Phasotron irradiation facility in JINR. That brought new ideas of calorimetric research due to the higher quality and stability of the 660 MeV proton beam and mostly its intensity, which is about two orders of magnitude higher than at Synchrophasotron.

Three unique experiments were performed during June 2017, May 2018, and June 2018. Natural

uranium target so-called Target Assembly QUINTA (QUasi-INfiniteTarget) consists of 298 identical cylinders where the metallic natural uranium is due to safety reasons covered by aluminum<sup>5</sup>. Cylinders' total dimensions (Fig. 1a) are 36 mm in diameter and 104 mm in length, including 1 mm of the alumina shell cover. Cylinders are fixed in five sections of hexagonal geometry (Fig. 1b-c) with total uranium mass equal to 512 kg. An aluminum plate with a thickness of 5 mm and a dimension of 350×350 mm covers each hexagonal section from the front and backside (Fig. 1d).

Due to the inconsistency of cylinders' connection with these plates, heat resistance is challenging to estimate. To investigate this phenomenon, a more straightforward experiment was performed. By this experiment, the precious analyzation of heat deposition inside of the cylinders is possible. Finally, another two targets are described in this paper. They were investigated by the purpose of searching for a new thick target usable for following experiments with 20 t depleted uranium subcritical blanket BURAN. Our team was observing several aspects, as surface neutron spectra, target heating density, or neutron flux dependence along the distance. Carbon and lead

\*Corresponding author (E-mail: svoboda@jinr.ru)

material were used with almost identical geometry of 19 cm in diameter and 100 cm length. The only difference between these targets was the number and length of cylinders the target was consisting of. For the Lead target, it was 5 cm long cylinders with a total quantity of 20 pieces, in contrast with the Carbon target where 10 pieces of 10 cm long cylinders were involved.

The temperature distribution was monitored online by precious thermocouples processed by National Instrument (NI) measuring card. The heat deposition was calculated by MCNPX 2.7.0 code<sup>6</sup> using the INCL4-ABLA physics models. Simulation results were used as input for Ansys Transient Thermal Analysis<sup>7</sup>. Activation analysis by various foils material was also involved at many positions on the targets, as on the surface, so inside. Foils were analyzed by the HPGe detector with the gamma-spectroscopy method to determine the neutrons and protons flux. Experimental data were also compared with simulated results by MCNPX. Anyway, these results are not included in this paper, as well as the research of the neutron and proton leakage. This part of the research is going to be submitted in further months. All the experiments were performed by the ADS research group at Dzhelapov Laboratory of Nuclear Problems at JINR.

## 2 Results and Discussion

Four experiments are described and discussed with focusing on the most complicated one, spallation target QUINTA and its cylinder irradiation. QUINTA has been used as a spallation target since 2011 and has been irradiated for several times, mostly to analyze neutron spectra in complicated geometry, its leakage, and energy gain. Heat generation monitoring is included in its research for the last three years. The first experiment was measured by only two thermocouples type K with tremendous uncertainty. Finally, due to the progress and implementation of more suitable thermocouples, its online calibration, temperature fluctuation compensation, and advanced

method of data analyzation, the experiment described in this paper uses 90 precious thermocouples with general uncertainty less than 1 %, even less than 0.5 % for about 90 % of applications. The combination of MCNPX and ANSYS simulation is still in developing mode.

Temperature measurement was carried out by thermocouples type T and E with gross gain about 4.279 mV and 6.319 mV per 100 °C, respectively. Thermocouples voltage was measured by the NI9214 and NI9212 convertors with cold junction compensation. All electronics were placed into a thermally insulated box to decrease adverse influences by temperature fluctuation of the surrounded air. The utilization of PT100 probes took care of online calibration. Probes were placed inside of the insulated measuring box with the NI9217 measuring card. It also monitors slowly increasing temperature caused by electronics heating with further utilization during advance data analyzation. Each thermocouple measures the temperature difference between the compensation of measuring card and fixed position on the experimental setup. Due to a radiation background in the experimental hall during the irradiation, the electronics were placed in a 20 m remote measuring room shielded by a 3 m concrete wall. The length of thermocouples is 21.5 m, and its dependence on accuracy of measurement was studied without negative conclusions.

Data are analyzed by *Python 3.7*<sup>8</sup> with using project interpreter *NumPy* and *pandas* for data analyzation, *SciPy* for signal analyzation with suppressing noise, *matplotlib* for charts plotting, and finally *PyCharm*<sup>9</sup> as an editor of codes.

### 2.1 Two cylinders irradiation

Two cylinders were situated in the axis of the proton beam with parameters shown in Table. 1. To determine heat deposition changes along the cylinder by MCNPX, each cylinder was in simulation divided into three equal pieces, as shown at the simulation of the setup (Fig. 2). Each piece of the cylinder was analyzed separately, as for spectra analyzation

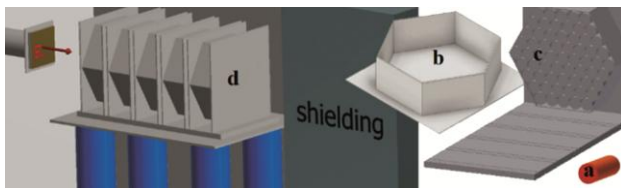


Fig. 1 — Quinta target, a) cylinder, b) hexagonal Al plate holder, c) section holder, d) the whole setup without Pb shielding.

Table 1 — Proton beam setting (660 MeV) with irradiation times

<i>Experiment</i>	$x, y_{center-shift}$ [cm]	$x_{FWHM}$ [cm]	$y_{FWHM}$ [cm]	$T_{irradiation}$ [min]	$I_{proton}$ [nA]
2 cylinders	0.16, 0.06	2.39	3.32	21.4	14.64
QUINTA	0.17, -0.09	2.16	2.74	314	12.93
Carbon	0.00, 0.09	3.51	3.46	254	21.03
Lead	0.06, 0.29	3.71	3.38	288	31.68

(Fig. 3), temperature measurement, and so for the heat deposition. Thermocouples were fixed to the cylinder by plastic insulation tape at the exact measuring position (Fig. 4). Proton spectra show the decreasing of both, as energy as flux. Due to this fact, analyzation of the heat deposition response is very important for both cylinders. Energy deposition by protons contributes to total heating by about 5.62 kJ, and it means about 78%. Heat deposition distribution of each cylinder part is described by Fig. 5. A vast number of particles escape from the cylinder target by depositing only a small fraction of usable energy or even none. This experiment is essential for understanding and describing the behavior of the cylinders inside of a more complex target QUINTA.

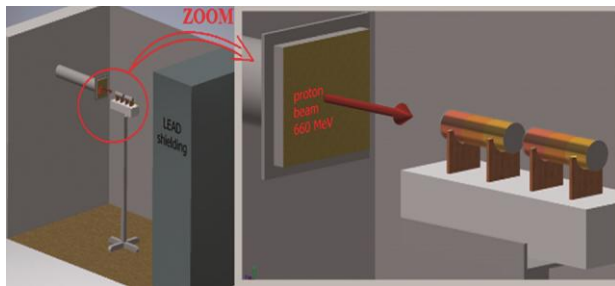


Fig. 2 — Two cylinders setup, illustration without cladding.

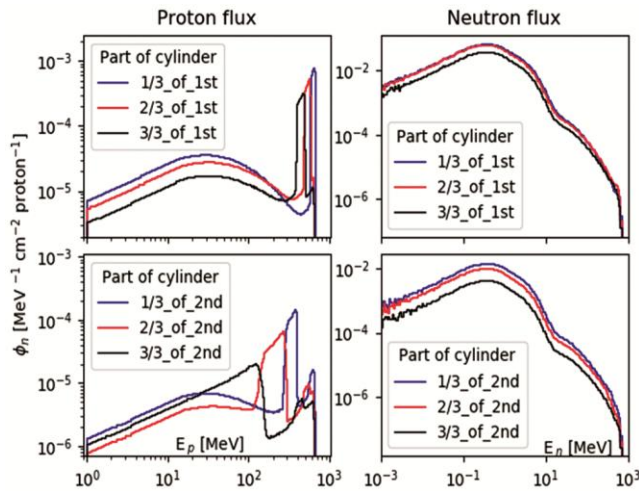


Fig. 3 — Calculated spectra for 2 cylinders exp. by MCNPX 2.7.0.

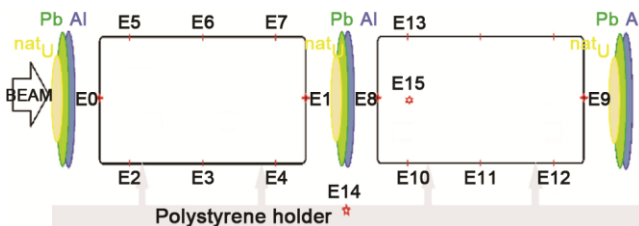


Fig. 4 — Measuring positions and labels of thermocouples with a description of activation foils.

Computed results by MCNPX were adapted as input data for ANSYS Transient Thermal Analyses software. The input parameter of heat power density [ $W \cdot cm^{-3}$ ] is the core of the whole simulation. Another crucial input for correct simulation is the setting of heat transfer parameters. The natural convection coefficient was determined for the exact cylinder geometry (Fig. 6) and the initial temperature difference between the simulated object and surrounded air temperature  $20^\circ C$ . To focus on the results of this experiment, the target was mostly heated by Coulomb heating from the slowing protons, negligibly by neutrons and gamma radiation. Subsequently, heating up by nuclear fission of  $^{nat}U$ . Comparing measured temperatures with ANSYS+MCNPX simulation for the first cylinder (Fig. 7), there is maximal front bottom temperature after 1260 s of irradiation  $E2 = 34.48(19)^\circ C$ , back bottom at  $E4 = 33.67(19)^\circ C$ , simulated  $E2_{calc} = 33.17^\circ C$  and  $E4_{calc} = 32.81^\circ C$ . Very important and challenging for experimental measurement with thermocouples is to set the offset and decrease all potential measurement uncertainties. The offset was setting by the E14 thermocouple placed on the insulated holder of cylinders (Fig. 4). The outside air temperature was

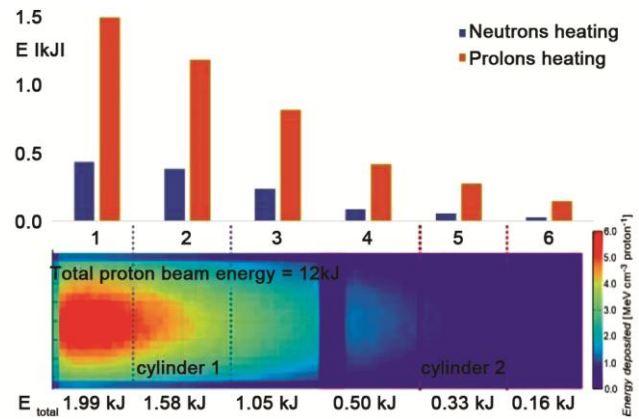


Fig. 5 — Energy deposition calculated by MCNPX.

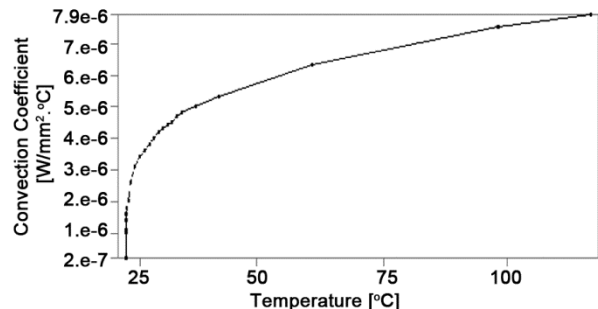


Fig. 6 — Natural convection of cylinder in  $20^\circ C$  air.

about 20.0°C and probes of PT100 compensate for the measuring box temperature fluctuations. The experimental uncertainty of temperature difference measurement is less than 1%. To estimate absolute temperature, the relative one (measured by thermocouples) is increased by compensation measured by PT100 thermometer in the measuring box with uncertainty not greater than 0.3%. To compare reference temperature (measured) with simulated one,  $\Delta E2 = 1.13(1)^\circ\text{C}$ ,  $\Delta E4 = 0.86(1)^\circ\text{C}$ , so relatively  $\delta E2 = 8.5\%$ ,  $\delta E4 = 6.7\%$ .

The front bottom temperature for the second cylinder (Fig. 8) after 1260 s of irradiation is  $E10 = 22.85(8)^\circ\text{C}$ , back bottom  $E12 = 22.70(8)^\circ\text{C}$ , for simulation  $E10_{\text{calc}} = 22.64^\circ\text{C}$  and  $E12_{\text{calc}} = 22.49^\circ\text{C}$  (Fig. 9). The error between these two methods is  $\Delta E10 = 0.21(1)^\circ\text{C}$ ,  $\Delta E12 = 0.21(1)^\circ\text{C}$ , so relatively  $\delta E10 = 7.3\%$ ,  $\delta E12 = 7.7\%$ . Due to the simulations of MCNPX and ANSYS are still in developing, it is expected that the uncertainty of these measurements will be slightly decreased in further months by simulation improving.

**2.2 QUINTA**

Beam shape is expecting to be in Gaussian distribution with parameters shown in Table. 1. Once

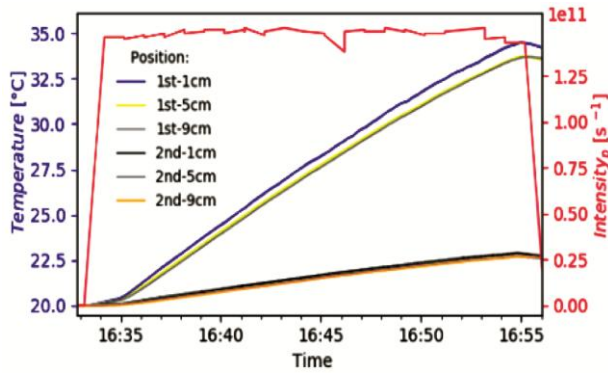


Fig. 7 — Experimental temperature measurement, both cylinder.

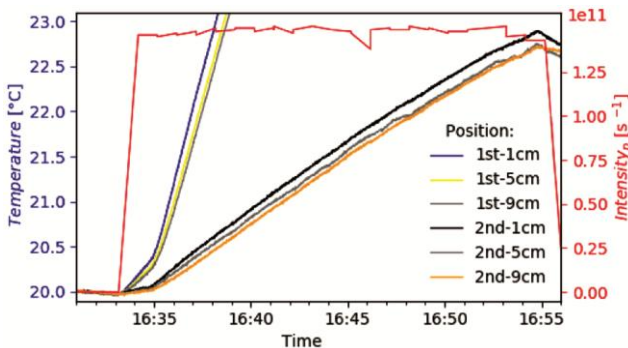


Fig. 8 — Experimental temperature measurement, cylinder 2<sup>nd</sup>

QUINTA contains the air gap (void) between the neighbors' cylinders, part of the proton beam goes through the whole target without interaction. To eliminate this phenomenon, QUINTA (meant axis z) is shifted (rotated) for angle 2° to the axis of the proton beam. When QUINTA irradiated, beam rotation is noticeable also in heat deposition (Fig. 10). There is shown how the heat deposition is slightly shifting to the left along the distance. Whole QUINTA is shown on the left side of the figure with the general scale of heat deposition normalized to an incident proton. On the right side, zoomed sections are shown separately with a different heat deposition scale for each one. According to MCNPX simulation, most of the heat (Fig. 11) was released in the second section due to

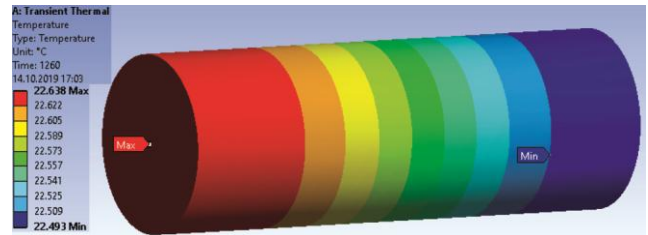


Fig. 9 — Simulation of second cylinder surface temperature.

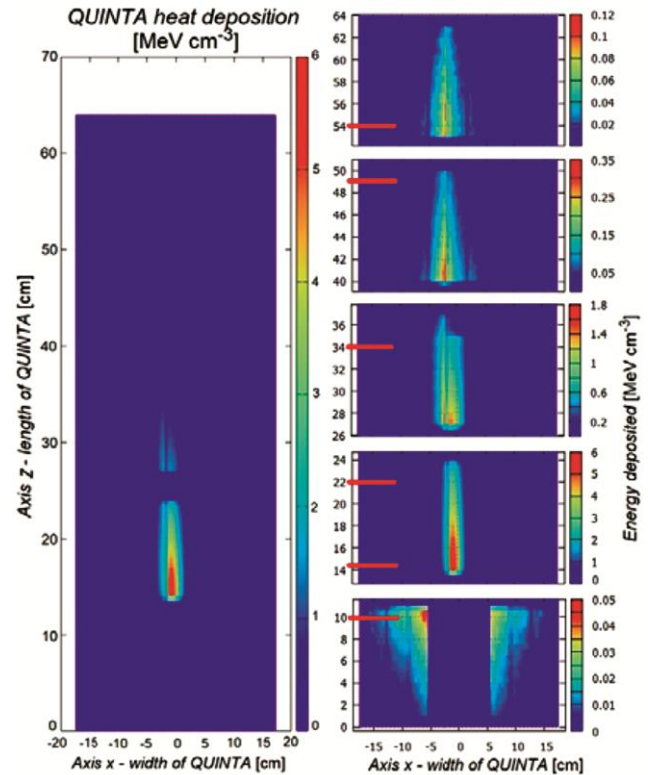


Fig. 10 — QUINTA heat deposition cross-section XZ (left) and XZ of the first section (bottom right), 2nd and consequently others (right upper), all normalized per proton.

slowing protons (69 kJ) and neutron fission (89 kJ). The kinetic energy of proton beam was in total 160 kJ, about 117 kJ was released by protons in QUINTA, and 180 kJ of heat generated neutron interactions, generally fission reaction. Due to the cylindrical geometry setup, many of neutrons and protons escaped from the spallation target.

Heat deposition dependency on the target length is described in Fig. 12 with cross-sections of *xy* axes and various “*z*” distance, marked in each figure. In the first

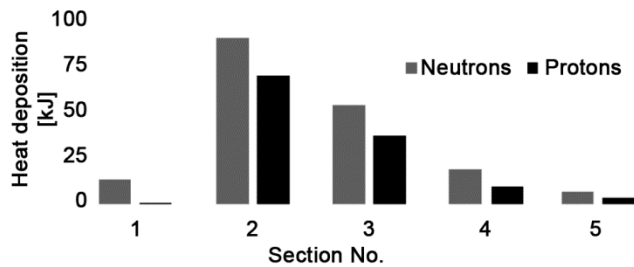


Fig. 11 — Heat deposition in QUINTA, MCNPX 2.7.0 simulation.

section, generally, all energy is generated by reflected neutrons, about 98%. Further section by section, the proton heat deposition is going to be less sharp, and the ratio of neutron heating to proton heating is increasing. For 2<sup>nd</sup>, 3<sup>rd</sup>, 4<sup>th</sup> and 5<sup>th</sup> section, 56 %, 59 %, 68 %, and 71 % is generated by neutron reactions respectively.

Experimental measurement was carried out by 88 thermocouples fixed on hexagonal alumina cover plates. Thermocouples were fixed at positions, as shown in Fig. 16 right, for both front and backside of each section. Due to the beam window of the first section, position 0,0 mm was not measured there. The sampling frequency of thermocouples measurement is set to be 1 s<sup>-1</sup> for all experiments. Fig. 13 shows measured differences in the center position (0,0 mm) of each section for both sides. Although the beam is nearly stable, in comparison with previous Synchrophasotron irradiation, some beam drops occur.

These drops are measurable by temperature decreasing activity. Interval of temperature drop is equivalent to the

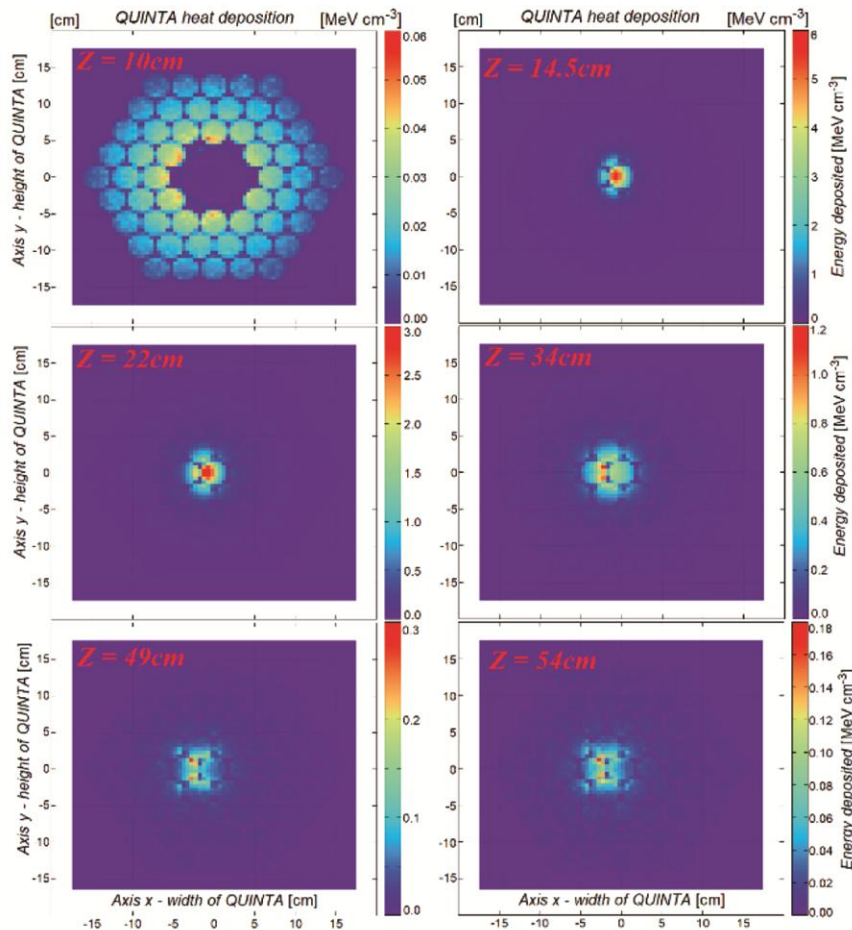


Fig. 12 — QUINTA cross-section XY heat deposition for various „*z*“ distance as red marks on Fig. 9, normalized per proton.

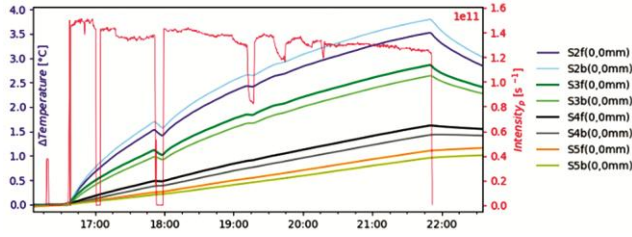


Fig. 13 — Temperature changes during irradiation for each section (S) for front side (f) and back side (b), except 1<sup>st</sup> one.

equivalent to the beam drop, without any detectable delays. The behavior of the beam is monitoring by Phasotron controlling room staff with frequency about 25 s<sup>-1</sup>, so, unfortunately, more precious observation of potential short delay is not possible. Red line at all of Fig. 13, Fig. 14, and Fig. 15 describes the intensity of the proton beam [s<sup>-1</sup>] with the scale on the right side. On the left side, axis represent temperature changes between the stable condition and irradiation for Fig. 13. Due to natural convection, upper parts are being heated

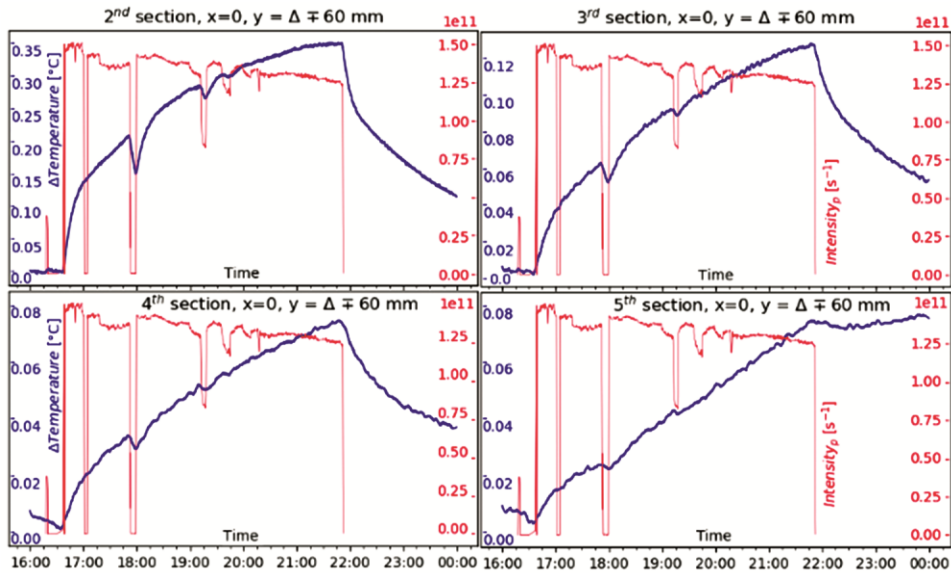


Fig. 14 — Temperature difference of position x,y (0,-60)-(0,+60) [cm], each section back side except first one due to beam window

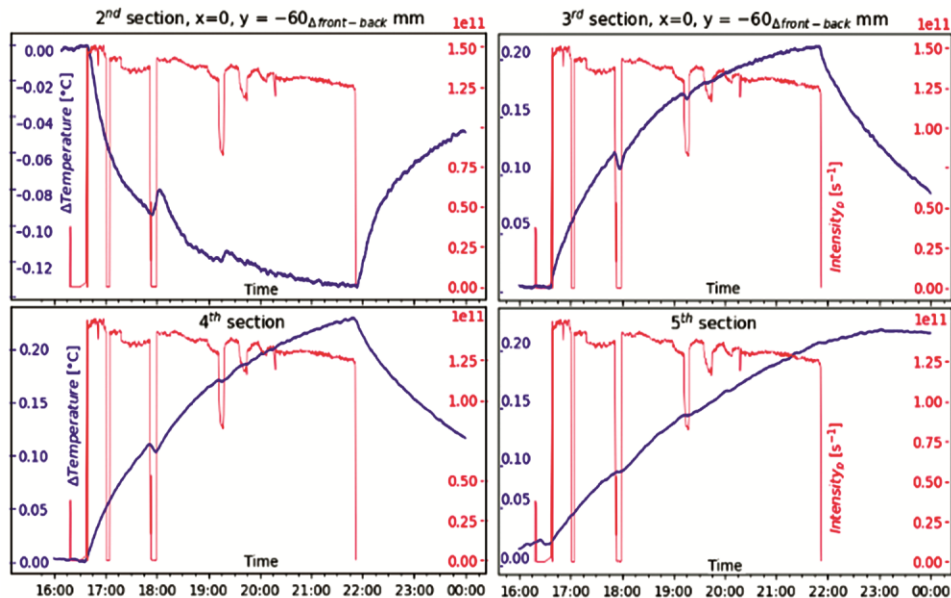


Fig. 15 — QUINTA temperature differences between front side and backside, measured positions x,y (0,-60) [cm]

up by lower ones as describes in Fig. 14, where compared positions  $y_1=+60$  mm with  $y_2=-60$  mm for  $x=0$  mm. Or slightly temperature difference  $\Delta T$  for  $T_{y1}-T_{y2}$  (Fig. 16, right – vertical difference). Finally, the heat generation decrease with distance along with the target, hence the measured temperature should follow this phenomenon. Figure. 15 shows it does not work for the second section. It is caused by the beam window in the first section, where natural convection is cooling the

front side of the 2<sup>nd</sup> section, and mostly the heat transfer by radiation is not reflected either generated from the opposite (backside of the 1<sup>st</sup>) section. This phenomenon (radiation transfer) is dependent on the absolute temperature of the 2<sup>nd</sup> section because of Stefan-Boltzmann's law. Due to only small temperature differences, it is just negligibly observed in Fig. 16, left.

**2.3 Carbon and Lead thick targets**

Heat deposition of these targets (Fig. 17) were also simulated in MCNPX and experimentally measured by thermocouples along the length. According to the threshold activation, the foil method has been found by our team that carbon produces much higher neutrons spectra with average energy up to 40-50 MeV in comparison with the lead target, generating about 10 times lower energy. According to the simulation, the Bragg peak for 660 MeV protons of Lead target has been located (Fig. 18, right, zoomed) at a distance 31.7 cm (including an air gap between 5 cm long lead cylinders). For Carbon target, protons go through the whole shape with length 104 cm (including 4 cm void). To find the Bragg peak, the more extended virtual target was calculated without void between cylinders. The Bragg peak was found in this case at 112 cm.

The shape of the proton beam along the target is gradually dispersing. The maximum heat deposition (Fig. 18, left) normalized to the incident particle is decreasing from  $0.4 \text{ MeV}\cdot\text{cm}^{-3}$  at 1 cm to

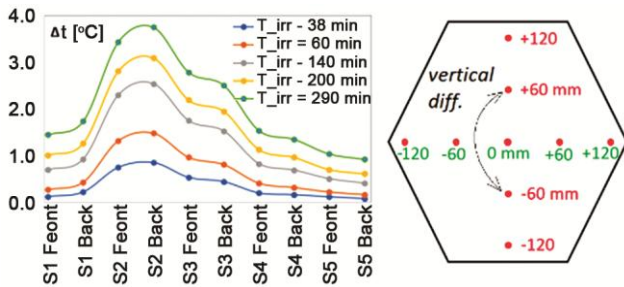


Fig. 16 — Temperature difference between stable state (left, before the irradiation start) to time of irradiation  $T_{irr}$ , position 0,0 mm, position description, where thermocouples placed



Fig. 17 — Thick targets of C and Pb setup

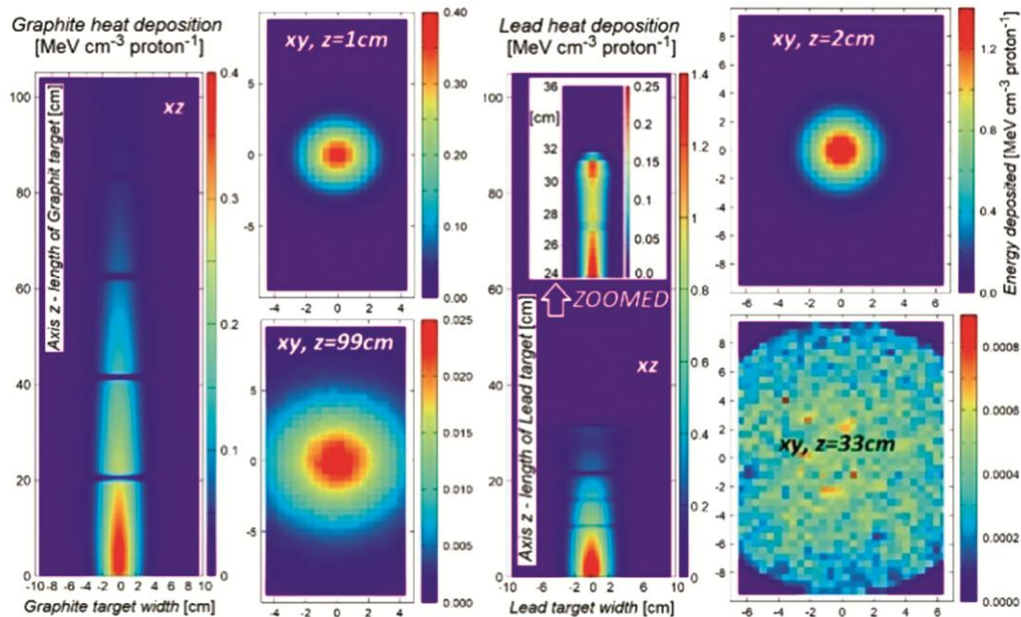


Fig. 18 — Heat deposition in Carbon and Lead target

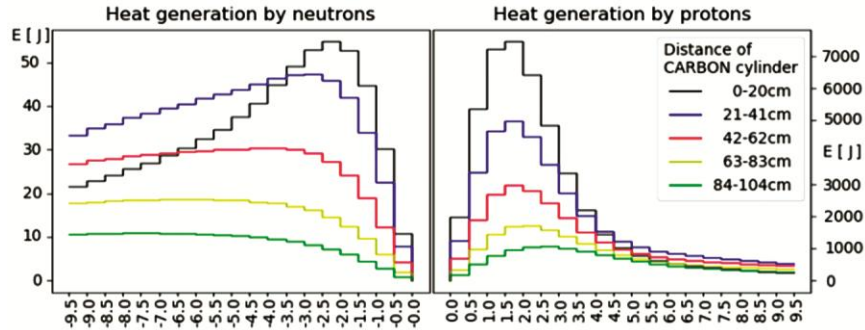


Fig. 19 — Heat generation dependency on radius distance, 5 mm rings

0.025 MeV·cm<sup>-3</sup> at 99 cm distance. To compare the dependence of heat deposition on the radius of the cylinder, other MCNPX simulation was calculated. Each cylinder consisted of an inner cylinder with radius 0.5 mm, surrounded by cylinder rings with increasing both of radius (inner  $r$  and outer  $R$ ) by 5 mm (annulus with inner radius  $r_{increased} = R_{previous}$  and  $R_{increased} = r_{increased} + 0.5$  cm). After normalization per gram, the highest density is in the center, with linear decreasing to the surrounded area. Total heat deposition by volume shown in Fig. 19, where both protons and neutrons heat deposition displayed. On the right side is shown proton deposition with more than 2 orders of magnitude greater scale than neutron deposition on the left side. During the irradiation, the beam was slightly unstable, and many beam drops occurred, as shown by the jagged temperature changes chart in Fig. 20. Irradiation of the Lead target is shown in Fig. 21, also, there is shown how the temperature reflects the beam drops (by jagged lines). As supposed after the Bragg peak, only heat background is measured due to heat transfer from heated parts.

### 3 Conclusions

Comparing temperature measurement by thermocouples with a combination of simulated results of MCNPX and ANSYS is challenging due to dealing with uncertainties in simulation as well as measurement. Experimental uncertainties were suppressed as describe at the beginning of the results. The combination of MCNPX with ANSYS and its uncertainties minimalization is still improving and developing. Inconsistent beam and its imperfect monitoring also play an essential role in quality simulation developing. Despite mention facts, the presented results are already in range of 10 % uncertainty between the experimental results to the simulated ones. The experimental equipment and its

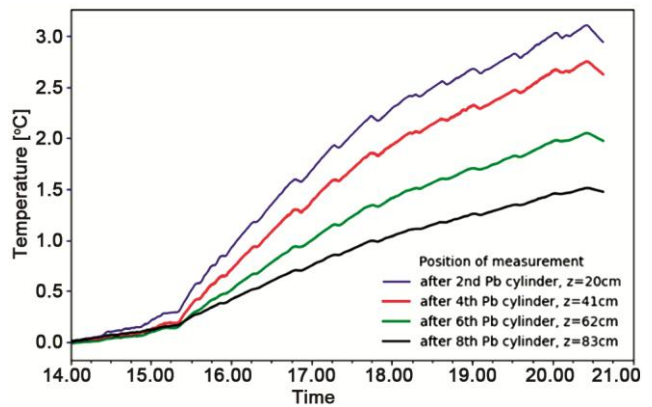


Fig. 20 — Carbon temperature differences in measurement

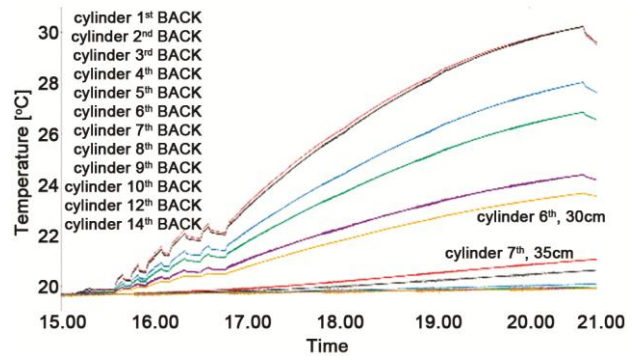


Fig. 21 — Temperatures at the back side cylinders of the Lead target

analysis already reached expecting goals. Higher computation capabilities for further simulations are required and already managed.

Comparing heat deposition simulated by MCNPX directly with experimental temperature data is tricky, but generally is describing the behavior of the targets. Temperature online monitoring by thermocouples is very cheap and offer many of measuring positions. Temperature measurement very accurately responds to beam changes, as shown at all measurement charts where beam drop causes the temperature drop without



any delays. Described methods and its developed application will be used for ADS subcritical blanket research as already planned in the ADS group in Dubna.

Generally, this research shows that the described temperature measurement follows the macroscopic heat effects inside of the observed targets. For simple geometry with known heat transfer parameters, is this method with 1 Hz responds describing very promptly inner processes.

### Acknowledgment

This research was partially supported by the Centre for Research and Utilization of Renewable Energy (CVVOZE). Authors gratefully acknowledge financial support from the Ministry of Education, Youth and Sports, and Ministry of Finances of the Czech Republic under the Inter-Excellence project No. LTT18021. The investigation was supported by the program of cooperation between the Czech Republic and JINR under the project 3+3-14/159/2018. Authors are very grateful to all Phasotron accelerator staff (JINR) for their work with

beam setting and controlling, to A.A. Baldin and I.I. Mar'in for their previous research with QUINTA target and their advices, and finally to R. Vespalec for his work on gamma spectroscopy analyzing software, help with experimental setup and advices during the research, all appointed from JINR.

### References

- 1 Batin V I, Batin D V & Borisov V V, et al, *JINR Rapid Commun*, 6 (1999) 35.
- 2 Tumendelger T, Chultem D & Krivopustov M I, et al, *JINR Preprint*, 247 (1999), Dubna.
- 3 Krivopustov M I & Chultem D & Adam J. et al, *JINR Preprint*, 168 (2000), Dubna.
- 4 Voronkov A V & Zemskov E A & Churbanov A G, et al, *KIAM Preprint*, 76(2000), Moscow.
- 5 Furman W I, Adam J & Baldin A A, et al, *PoS (Baldin ISHEPP XXI)*, 086 (2012).
- 6 Pelowitz D B, MCNPX version 2.7.0, User Manual, LA-CP-11-00438, 2011.
- 7 ANSYS® Transient Thermal Analysis, Release 16.0
- 8 Python Software Foundation. Python Language Reference, version 3.7. Available at [www.python.org](http://www.python.org).
- 9 JetBrains (2017). PyCharm. JetBrains. Available at: [www.jetbrains.com/pycharm](http://www.jetbrains.com/pycharm).